Present and Future of Modeling Global Environmental Change: Toward Integrated Modeling, Eds., T. Matsuno and H. Kida, pp. 221–241.

Ice in the Climate System: Paleoclimatological Perspectives

W. R. PELTIER and L. P. SOLHEIM

Department of Physics, University of Toronto, Toronto, Ontario, Canada M5S 1A7

Abstract—The impacts of the distributions of land ice and sea ice on planetary climate are extremely important, both regionally and globally. The clearest possible appreciation of this fact derives from a comparison of modern climate with the climate of the Last Glacial Maximum at 21,000 years before present (BP). The analysis of LGM climate described in this paper is based primarily upon a new sequence of numerical simulations that have been performed with the Climate System Model (CSM) of the National Center for Atmospheric Research (NCAR). These analyses are apparently the first to attempt to obtain a new statistical equilibrium solution for a complete coupled atmosphere-ocean model for this epoch of time. Intercomparisons of the results of the new CSM integrations are described with a number of previous analyses that employed a variety of different models and modelling strategies.

INTRODUCTION

The use of modern atmosphere-ocean general circulation models to investigate climates of the past (paleoclimates) has been motivated to significant degree by the need to test the robustness of these models under conditions which differ markedly from present. Given the fact that critical subgrid-scale processes in these models, such as deep convection in both the atmosphere and oceans, must be parameterized, there is no guarantee that the representation of them will remain applicable in conditions that differ from the modern conditions to which the parameterization schemes are tuned. By simulating climates of the distant past in epochs from which there exists a sufficient quantity and quality of proxy climate information that reasonable reconstructions of climate state are possible, analyses of this kind may be extremely useful. If the models of the climate system that we employ to make predictions of future climate states that will obtain under conditions of enhanced greenhouse gas forcing fail such paleoclimate tests, we would be obliged to be concerned as to the validity of their predictions for the future. The epoch of choice for such analysis, because of the magnitude of the international effort that has been focused upon it, is the most recent period during which the Earth experienced a significant increase in the extent to which its surface was glaciated. This period is referred to as Last Glacial Maximum (LGM) and occurred approximately 21,000 calendar years before present. It is the period that will serve as focus of the new analyses to be described herein.

This period of maximum extent of glaciation was simply the most recent of the quasi-periodic sequence of advances and retreats of the northern hemisphere continental ice-sheets that commenced in mid-Pleistocene time approximately 900,000 years ago. Each such glacial cycle, which was characterized by a relatively slow glacial advance on a timescale of approximately 90,000 years and a relatively rapid retreat on a timescale of approximately 10,000 years, therefore lasted approximately 100,000 years (see Peltier (1998a) for a recent review). On the basis of oxygen isotopic data from deep-sea sedimentary cores, shown by Shackleton (1967) to be an excellent proxy for continental ice-volume, it has come to be well understood that this cycle of glaciation and deglaciation was a response of the climate system to the small changes in the effective intensity of the Sun that are caused by time variations in the geometry of Earth's orbit (Hays *et al*., 1976). It is a consequence of gravitational n-body effects in the solar system that the obliquity of the spin-axis (the angle it makes with the plane of the ecliptic) as well as the eccentricity of the orbit, are caused to vary quasi-periodically in time. The former of these two geometric properties of the Earth's orbit varies with a characteristic period of 41,000 years whereas the latter varies with characteristic periods of 100,000 and 400,000 years. It was the central thesis of Milankovitch (e.g. 1941) that the influence of these changes upon the seasonal variations of solar insolation was the cause of the ice-ages, a fact that was essentially confirmed by Hays *et al*. (1976). Although it has proven difficult to construct an a-priori model of the 100 kyr glaciation cycle, since strong nonlinearity must be involved and the timescale is far too long to allow conventional atmosphere-ocean general circulation models to be employed, significant recent progress has been achieved based upon the use of models of intermediate complexity (see Tarasov and Peltier (1999) and Marshall *et al*. (2000) for recent examples of work of this kind).

Rather than discussing the physics of the 100,000 year glaciation-deglaciation cycle of the late Pleistocene epoch, our purpose here will be to investigate the properties of the climate state that obtained at LGM. To this end we will begin in Section 2 by comparing a number of simulations of LGM climate that have recently been performed in the context of the Paleoclimate Model Intercomparison Project (PMIP). These simulations were all performed using identical conditions of solar forcing, atmospheric carbon dioxide concentration and land-ice distribution and paleotopography, and so one might have reason to hope that the different models would deliver climate predictions for the LGM epoch that were extremely similar to one another. Following a discussion of the boundary conditions themselves, we demonstrate that there are in fact very large discrepancies between the predictions of the PMIP suite of models for the LGM period. We then proceed in Section 3 to describe the new sequence of simulations that we have performed with the NCAR CSM version 1.2 running in low spatial resolution paleoclimate mode. For the purpose of these integrations we have also included the minor modification to the ice-sheet component of the paleotopography due to the influence of "implicit ice " as described in Peltier (1998b).

These analyses will explore the utility of a method to accelerate the

convergence of the deep thermohaline circulation of the oceans in order to achieve a statistical equilibrium state for the coupled climate system under LGM conditions. It proves interesting to compare the properties of LGM climate predicted by the NCAR CSM to those delivered by the PMIP set of models. A summary of our results is offered in the concluding Section 4.

INTERCOMPARISON OF THE PMIP SUITE OF SIMULATIONS OF LGM CLIMATE

The Paleoclimate Model Intercomparison Project (PMIP), described in detail by Joussaume and Taylor (1995), has chosen two fiducial epochs as focus, respectively the mid-Holocene warm period at 6 kyr before present and the LGM it 21,000 years BP. Unlike the orbital radiation regime that existed in mid-Holocene time, that which existed at LGM did not differ significantly from present and is illustrated in Fig. 1. As is clearly evident on the basis of CO_2 measurements in air bubbles in the Vostock ice-core (Barnola *et al.*, 1987), the concentration of this well mixed trace gas at LGM was very close to 200 ppmv and thus significantly lower than the pre-industrial level of 280 ppmv. By far the most significant change in boundary conditions at this time, however, was that associated with the land-sea distribution and the topography of the planet with respect to sea level, especially associated with the contribution to paleotopography due to the presence of the ice-sheets that were in place over Canada and Northwestern Europe. As well as constituting important modifications to topography, these ice-sheets of course had significant thermal impact because of their high albedo.

Global models of LGM paleotopography and land-sea mask that fully incorporate the influence of the lowering of sea level due to the removal of water from the global oceans that was required to build the ice-sheets, as well as the dramatically increased elevation of the ice-loaded regions of the continents, were most recently refined by analyses reported in Peltier (1994, 1996) based upon the use of the global theory of the glacial isostatic adjustment process (Peltier, 1974, 1976; Peltier and Andrews, 1976; Farrell and Clark, 1976; Clark *et al.*, 1978; Peltier *et al.*, 1978; Wu and Peltier, 1982, 1984; Tushingham and Peltier, 1991, 1992; Mitrovica and Peltier, 1991). The structure of this theoretical model, which has come to be widely employed by many groups internationally, is embodied in an integral equation for relative sea level history that I refer to as the Sea Level Equation (SLE). Given a history of the variations of the thickness distributions of the continental ice-sheets, and a model of the radial variation of mantle viscosity, the solution of this integral equation predicts the time dependent separation of the surface of the sea (the geoid of classical geodesy) and the surface of the solid Earth. In Peltier (1994) it was shown how this linear perturbation theory based analysis could be made topographically self-consistent and thereby enable one to make a detailed prediction of the time-dependence of the topography of the entire planet from LGM to present. This analysis also delivered an accurate prediction of the variation in the position of coastlines everywhere on the Earth's surface as once ice-covered regions rose out of the sea as a consequence of crustal

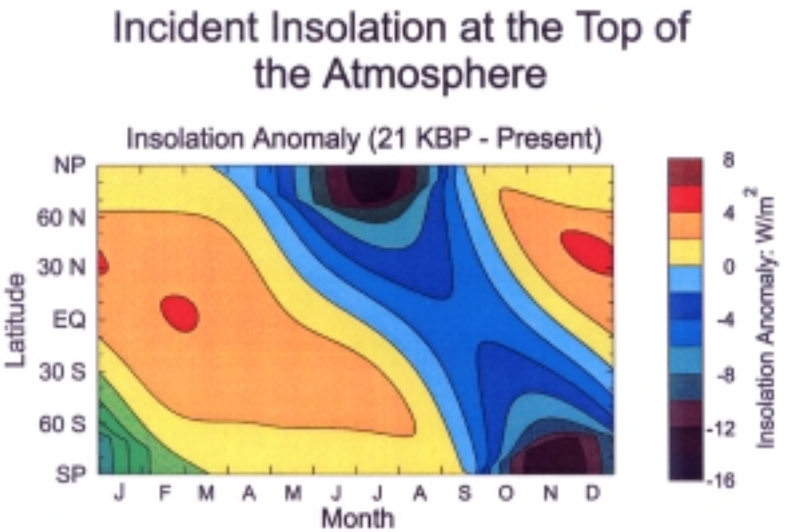

21 KBP Orbital Parameters

Present Day	
Eccentricity:	1.6720 %
Obliquity:	23.446 Degrees
Longitude of Perihelion:	102.04 Degrees
21000 Years BP	
Eccentricity:	1.8994 %
Obliquity:	22.949 Degrees
Longitude of Perihelion:	114.42 Degrees

Fig. 1. The insolation regime at 21,000 years before present presented in the form of a latitude and month of year deviation from that which obtains at present. Also shown is a comparison between the values of the orbital parameters at present and those at 21,000 years ago.

rebound and as low lying regions became inundated by the sea as the continents deglaciated and mean sea level rose through the addition of glacial meltwater to the ocean basins.

Figure 2 shows the Northern Hemisphere and Southern Hemisphere distributions of land-ice, sea ice, and the land sea distribution at LGM as defined by the ICE-4G (VM2) model of Peltier (1994, 1996, 1998b). The large Northern Hemisphere ice-sheets that covered Canada (the Cordilleran, Laurentide and Innuitian complexes) and Northwestern Europe (the Fennoscandian, Barents Sea

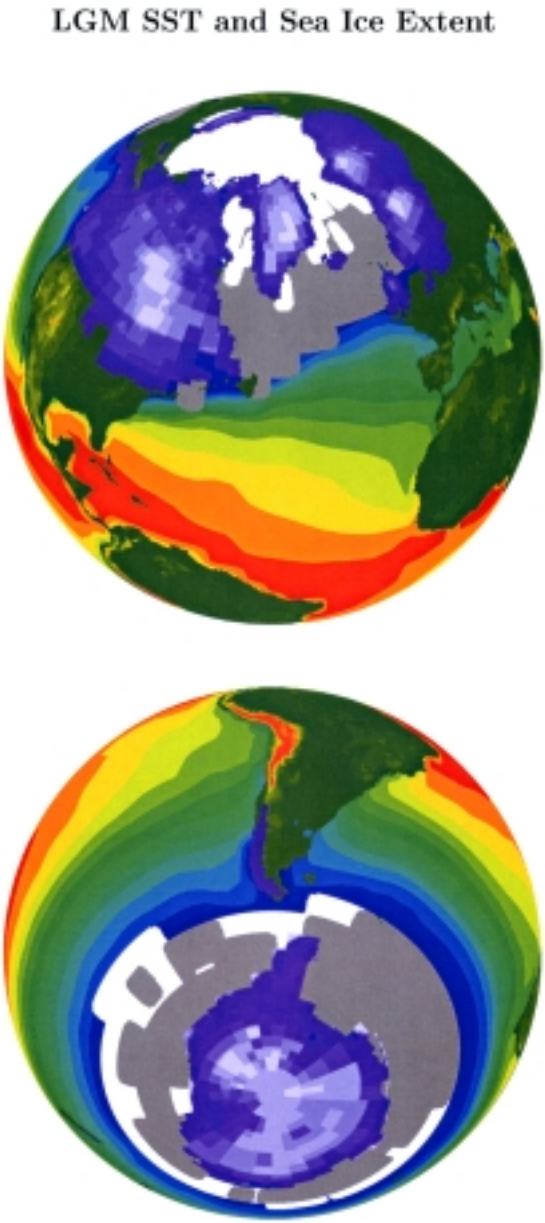

Fig. 2. Northern and Southern Hemisphere satellite views projections of the distributions of land-ice and sea-ice at LGM 21,000 calendar years ago. The distribution of sea ice in Northern Hemisphere summer (Southern Hemisphere winter) is shown as white whereas the Northern Hemisphere winter distribution is shown as the grey scale extension. The land ice distribution is based upon the ICE-4G model of Peltier (1994). The annually averaged sea surface temperature distribution is shown as the colour contoured overlay on the ocean basins. These results are those delivered by the fully coupled NCAR CSM.

and Kara Sea complexes) together with the smaller Patagonia, British Isles and Iceland complexes, are clearly evident. Also shown on this figure, by an overlay over the ocean basins, is the distribution of sea surface temperature (SST) that is predicted by the CCC2 model under these LGM conditions and which will be a focus of discussion in later sections of this paper. By the white and grey regions we also illustrate the summer and winter sea ice extents under LGM conditions from the same model. We note furthermore the existence of the land bridge which then connected the British Isles to the European Mainland because of the exposure of the floor of what is now the English Channel. Detailed graphical illustrations of the other land bridges that existed at that time were provided in Peltier (1994). Another of the more important exposures of continental shelf during the LGM epoch is evident on the southern hemisphere perspective of Fig. 2 to the east of present day Argentinian Patagonia, where the Argentine shelf was exposed as far outboard of the present coastline as the Falkland Islands (a more detailed map of this exposure, which is believed to have been an important source of the terrigenous dust that was deposited during glacial intervals in the Vostock ice-core, will be found in Rostami *et al*. (2000)).

Figure 3 shows a summary of results from the subset of the models that have performed the PMIP set of mandated LGM experiments, all of which employed the above described set of boundary conditions. These were very simple experiments based either upon the use of fixed SST's determined by the maps of this quantity inferred by the CLIMAP (1976) group, even though these are now known to be suspect in many regions (e.g. see Hostetler and Mix, 1999), or upon the use of models that compute SST's by coupling the model of the atmospheric general circulation to a mixed layer model of the oceans in which heat fluxes are specified so as to allow the model to fit modern observations of SST and sea ice extent. In the mixed-layer coupled models, these heat fluxes are assumed not to change under LGM glacial conditions, the implication being that the ocean general circulation was not significantly different from modern in either its wind-driven or thermohaline components. Inspection of the results for this simple set of PMIP experiments, which are shown on Fig. 3 in the form of plots of LGM tropical sea surface temperatures and sea surface temperature anomalies as a function land surface temperatures and land surface temperature anomalies, all zonally averaged between 30°N and 30°S latitude, demonstrates the extremely large discrepancies between the LGM predictions of the subset of the PMIP models which have been employed to perform the two experiments. On the basis of what should be the more accurate analyses of LGM paleoclimate, namely those performed using the mixed layer ocean versions of the various models, there is a difference of almost 3°C between the warmest (UGAMP) and the coldest (the Canadian Climate Center model CCC2) models of the mean SST's over the tropical oceans. The NCAR Community Climate Model (CCM1) is very close in its predictions of both tropical SST's and ground temperature in the tropical belt to the predictions of the CCC2 model.

One apparently robust conclusion that follows from the PMIP LGM reconstructions, however, is that (with the exception of the UGAMP model) the

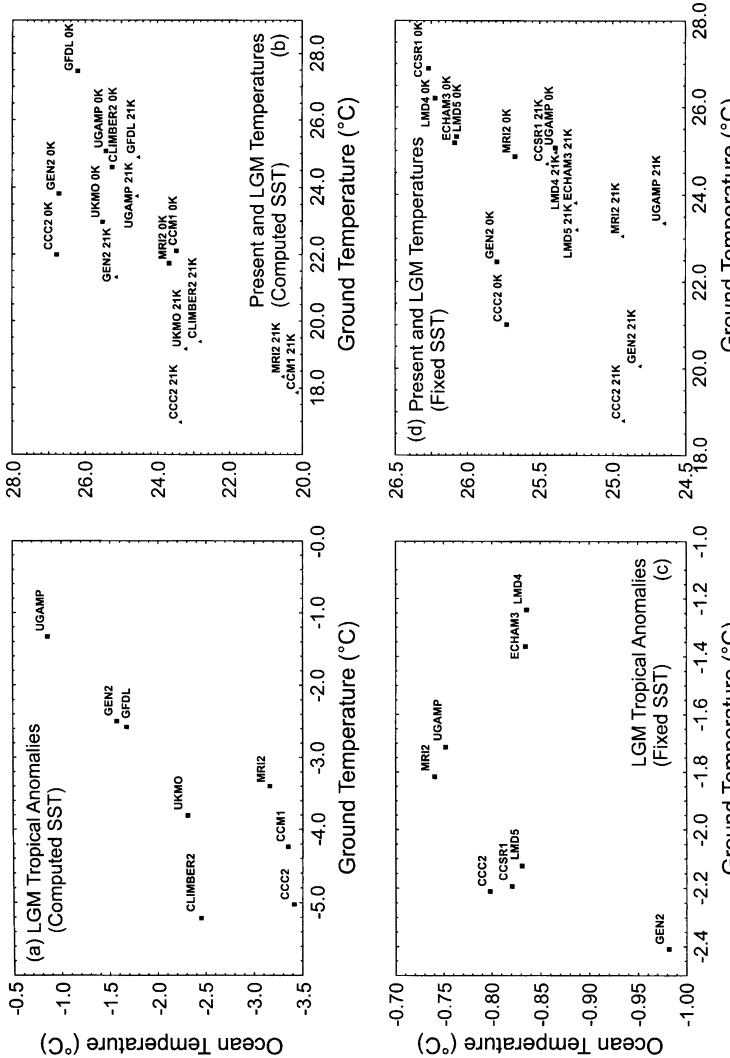

Fig. 3. PMIP differences in tropical ground temperature versus tropical ocean SST's between 30°S and 30°N. (a) LGM-modern tropical land and ocean differences in the computed SST PMIP experiments. (b) Present and LGM tropical temperatures for the computed SST experiments. (c) LGM-modern tropical land and ocean differences in the CLIMAP fixed SST PMIP experiments. (d) Present and LGM tropical temperatures for the fixed SST experiments.

predicted tropical SST's are significantly colder in the mixed layer ocean versions of the models then they are when CLIMAP fixed SST's are employed. In the recent past there has of course been a great deal of effort expended, using a variety of proxy indicators, to infer the LGM distribution of SST, not only in the tropics but also globally. As demonstrated by the above described CLIMAP fixed SST set of PMIP experiments, a very small degree of tropical cooling is consistent with the reconstructions produced by CLIMAP which were based upon the use of assemblages of foraminifers. More recent, however, reconstructions based upon alkenones have been characterized by a more significant degree of cooling of approximately 2°C, which was quite uniform, somewhat more than double the predictions of the CLIMAP fixed SST set of models (Bard *et al*., 1997). Other estimates, based upon the measurement of Sr/Ca isotopic ratios in corals (Guildersen *et al*., 1994), however, and on noble gas measurements (Stute *et al*., 1995), have suggested even larger tropical cooling as great as 5°C. More recent analyses, that allow for the influence of pore water ice volume (Schrag *et al*., 1996) and pH (Spero *et al*., 1997), based upon oxygen isotopic inferences, have been argued to be closer to the colder estimate of a 5°C cooling than to the alkenone derived result. Additional evidence that favours this greater degree of cooling has also been inferred on the basis of tropical snow line depressions (Rind and Peteet, 1995; Broecker, 1997; Thompson *et al*., 1995). On the basis of part (a) of Fig. 3, it will be clear that the coldest model in the PMIP set, namely the Canadian Climate Centre CCC2 model, together with the NCAR CCM1 model and the MRI2 model of the French group, come closest to fitting the coldest of the inferred tropical LGM temperature depressions. These predictions lie mid-way between the alkenone derived results and those delivered by the coral based SST proxy.

LGM CLIMATE RECONSTRUCTIONS USING THE NCAR CSM1.0 COUPLED CLIMATE MODEL

Since climate models based upon the coupling of a mixed layer representation of ocean heat transports to a model of the atmospheric general circulation do not properly describe the former, even though they are designed so as to enable the coupled model to fit modern day observed SST's and sea ice extents, it is clear that such models cannot be expected to deliver accurate predictions of SST's under the dramatically different conditions of radiative forcing and surface boundary conditions that obtained at LGM. It is therefore sensible to enquire as to the differences that might exist between the LGM predictions of such models and those that would follow from application of a full coupled model of the three dimensional circulations of the atmosphere and oceans together with sea ice dynamics and land surface processes to the same interval of time. To this end, we have been employing the paleoclimate version of the NCAR CSM in which the atmospheric circulation is described pseudo-spectrally at T31 with 18 vertical levels and the ocean is described at $3° \times 3°$ horizontal resolution using 25 vertical levels (a complete description of the standard higher resolution version of the NCAR CSM will be found in the June 1998 issue of the Journal of Climate). Space

will not allow us to review the details of this model here, nor is this necessary given the very detailed description available in the above referenced special publication. We simply note that it is evidently one of the best of the existing models in its class. In applying it to simulate the climate of the LGM epoch, we further note at the outset that our goal is to develop a simulation in which the ocean general circulation is statistically equilibrated with respect to both its wind driven component and its thermohaline component. Although the former will equilibrate quickly under the imposed LGM boundary conditions, the latter is characterized by such long governing timescales that it would be prohibitive to integrate to statistical equilibrium without recourse to special methods. One of the many useful characteristics of the CSM, however, is that it is possible using it to accelerate the convergence of the deep thermohaline contribution to the equilibrium climate by employing a "stretched timestep" for the deeper oceanic layers such that the stretching is a function of ocean depth. By invoking this methodology we have been able to employ a spin-up time for the abyssal ocean of 2500 years and thus have reasonable hope that our LGM simulation is close to statistical equilibrium with respect to both its wind driven and thermohaline components. LGM results predicted by several versions of the NCAR CSM are illustrated on Fig. 4 for the "spin-up" to equilibrium, including results for the two configurations mandated under PMIP as well as those obtained using the complete atmosphere-ocean coupled version of the model.

For the modern circulation, spin-up results for which are labelled 2 and 4 for the fixed SST and mixed layer ocean versions of the model respectively, both versions of the model deliver an annually and surface area averaged air temperature near 14.50°C which is well within error of the result delivered by modern observations. That the mixed layer ocean and fixed SST results are essentially identical is not surprising since the mixed layer ocean version of the model has ocean heat fluxes tuned to the modern observed sea surface temperature and sea ice fields. For LGM, climate spin-up results are shown for fixed SST (CLIMAP, curve 1), mixed layer ocean (curve 3), and for two versions of the full coupled CSM, each of which has been "initialized" in slightly different ways. The curve labelled 5 was delivered with the CSM running in the full synchronously coupled mode for a timescale of 80 years. Curve 6 was delivered by 50 years of full synchronous integration following 50 years of integration run by applying accelerated convergence for the deep ocean such that the abyssal waters experienced the equivalent of 2500 years of evolution, the initialization of the latter run having been based upon the final state delivered by the 80 year initial full synchronous integration.

Inspection of the LGM results on this figure will show that the mixed layer ocean and fixed SST simulations of LGM conditions appear to equilibrate at approximately the same value of annually averaged and spatially averaged mean surface temperature near 10.75°C, implying an LGM depression of approximately 3.75°C. The full synchronous 80 year integration of the CSM without the use of accelerated deep ocean convergence has not fully equilibrated by the end of the integration period but appears to continue to drift to lower temperature. By the

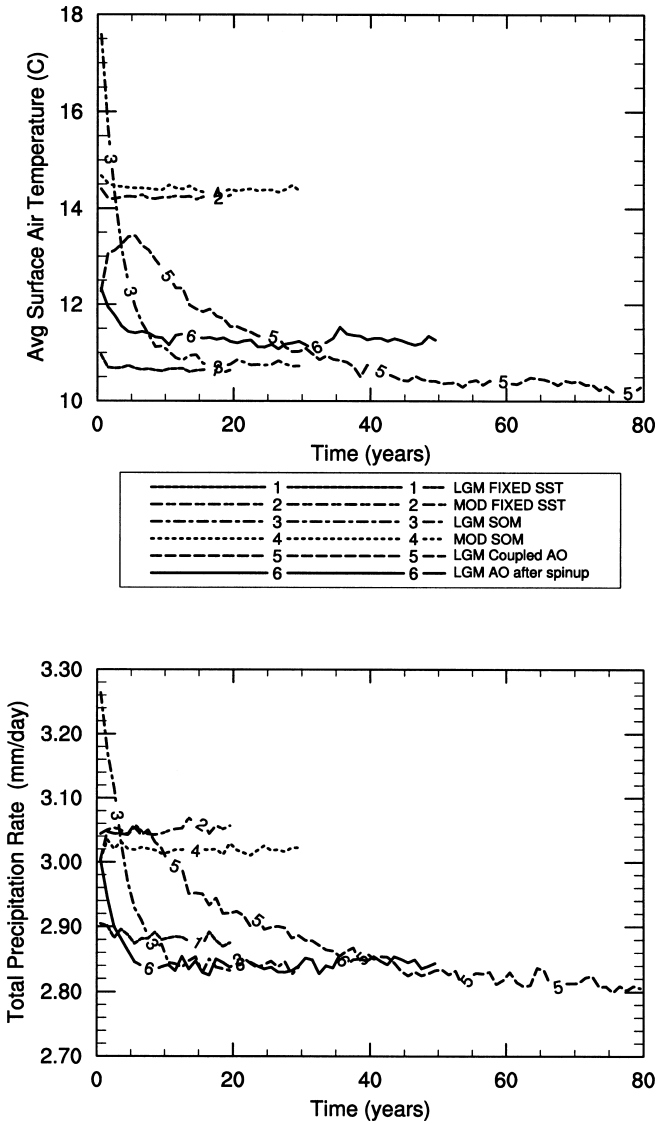

Fig. 4. Mean surface temperatures and precipitation rates during the spin-up of the six different versions of the NCAR CSM model discussed in this paper.

end of the run the mean surface temperature is approximately 10.25°C implying a degree of global cooling of approximately 4.25°C. It is unclear at what mean surface temperature the run would equilibrate if it were to be continued for a time sufficiently long to deliver a fully equilibrated deep circulation. When the climate solution that obtains at the end of this 80 year integration is employed to initialize

the version of the model which employs accelerated convergence for the deep ocean, inspection of curve 6 in Fig. 4 shows that the ensuing integration equilibrates at a value of mean surface temperature near 11.5°C thus corresponding to a reduced glacial cooling of approximately 3°C. In assessing the meaningfulness of the latter result, however, it is important to understand that the scheme employed to accelerate convergence of the deep ocean in the CSM does not precisely conserve energy and it could well be that the reason why this version of the model delivers a somewhat warmer LGM climate than the full synchronous integration is connected with this problem. Although it would be possible to modify the model in an ad hoc way to correct for violation of thermal energy conservation, analyses of this kind will not be discussed here. Figure 5 shows equivalent spin-up results for these six versions of the CSM in terms of the annually and spatially averaged precipitation rate, inspection of which demonstrates that this measure of the vigour of the hydrological cycle decreases significantly from present to LGM, as one would expect simply on the basis of the fact that colder air can hold less water vapour. The mean annual precipitation rate falls from a value of approximately 3.05 mm/day to a value of approximately 2.8 mm/day, a drop of approximately 8%. These results for the hydrological cycle are in reasonably close agreement with those obtained using the simpler CCC2 model (Vettoretti *et al*., 2000).

It is interesting to note, however, that the LGM depression of the average surface temperature is somewhat lower than the average ground surface temperature depression delivered by even the coldest (CCC2) model in the PMIP set for which results were shown on Fig. 3. Prior to discussing the modification to the LGM simulation that is produced through the integration to equilibrium of the deep thermohaline component of the circulation, we will proceed to describe one detailed property of the circulation delivered by these models that has not been described previously. This concerns the impact of the “implicit ice ” component of the surface topography (Peltier, 1998b) on the LGM circulation.

To this end, Fig. 5 shows the LGM paleotopography delivered by the ICE-4G (VM2) model of Peltier (1994, 1996) both including and excluding the contribution due to “implicit ice ” as well as the difference. Higher resolution regional versions of these data sets are shown in Peltier (1998b). In Fig. 5 the fields are shown projected on the T31 truncated basis of spherical harmonics employed to define model fields in the paleoclimate version of the NCAR CSM. Inspection demonstrates that the enhancements of model topography produced by the incorporation of implicit ice are localized to those regions that were initially covered by continental ice-sheets but later came to be inundated by the sea. Such regions are restricted primarily to Hudson Bay and the Barents and Kara Seas, and to a lesser extent to the Gulf of Bothnia which served as the centre of the Fennoscandia ice-sheet. Figure 6 shows results from the LGM fixed SST version of the CSM on which we have superimposed the annually averaged maps of surface air temperature and the surface wind arrows for both simulations that include and that exclude implicit ice and for the difference fields. Inspection will show that the net impact of the implicit ice enhancement of the paleotopography

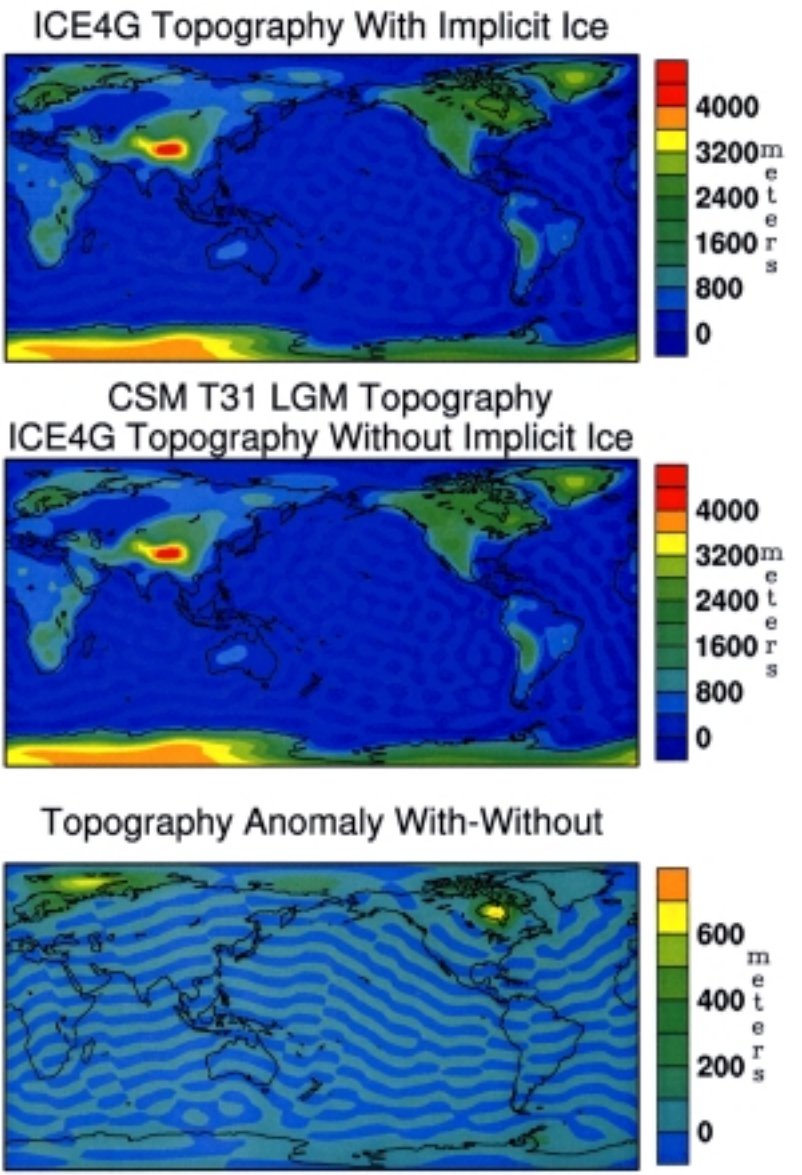

Fig. 5. The "implicit ice " contribution to LDM topography projected onto the T31 spectral grid employed in the paleoclimate version of the NCAR CSM.

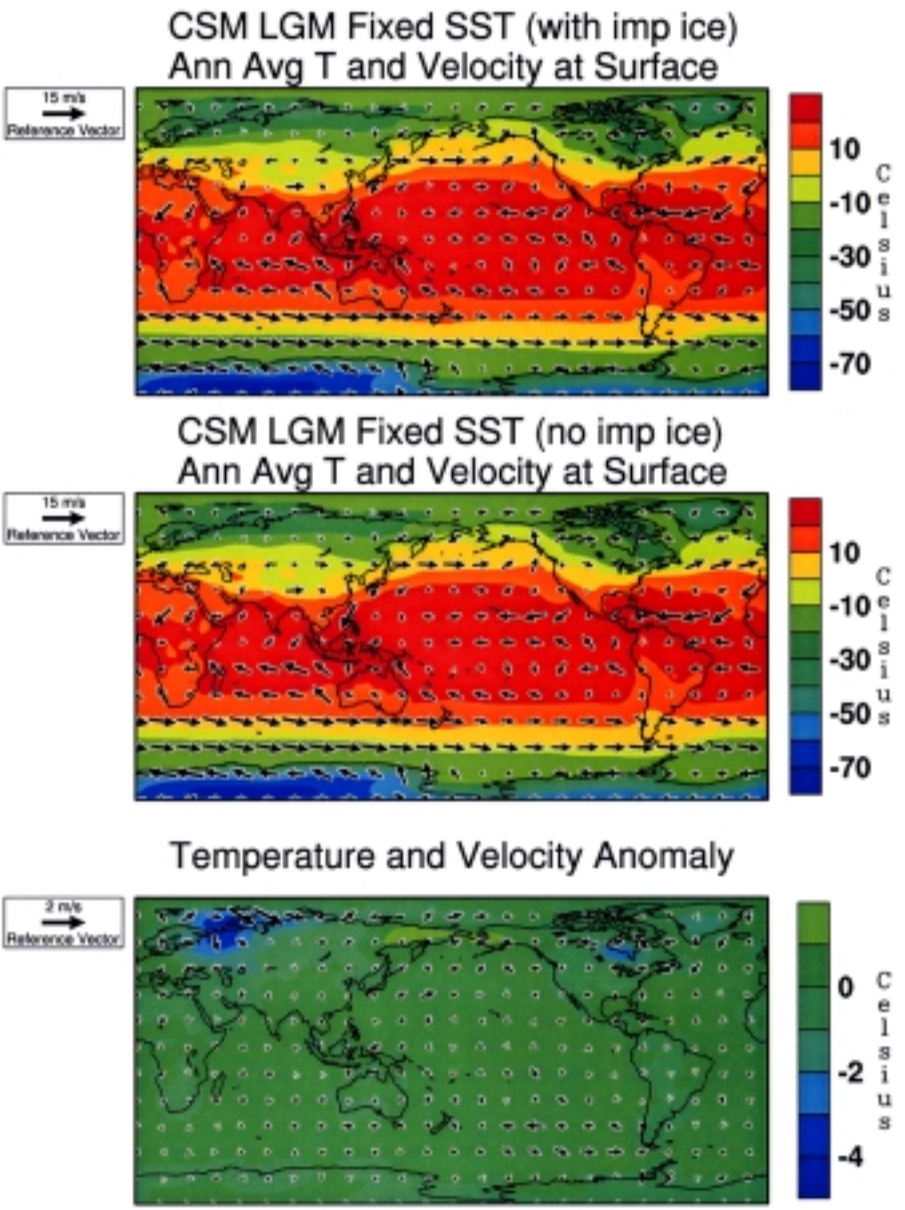

Fig. 6. The impact on mean surface temperature and surface winds of the “implicit ice” comment of the surface topography shown on Fig. 5.

over the ice-sheet centres is to slightly enhance the anticyclonic circulations that form over these surface cryospheric structures and to slightly enhance the degree of surface cooling by maximum amounts of approximately 3°C in highly localized regions.

As mentioned in Section 2 of this article, it is of special interest to enquire as to the degree of cooling of the tropical ocean that was characteristic of LGM conditions. The new sequence of LGM simulations that we have performed using the CSM has enabled us to address this issue using a variety of different model configurations. Figure 7 shows the zonally averaged sea surface temperature field between –30°S latitude and +30°N latitude for the modern ocean based upon Levitus data (curve 5), together with LGM predictions of the same field derived from a number of simulations of the climate of this epoch, only 2 of which are CSM based. Curve 1 is the CSM prediction for this field based upon the use of CLIMAP fixed SST's. Curve 4 is the result obtained from the 80 year synchronously coupled run of the complete CSM. Comparing the latter two results it will be clear that the fixed CLIMAP SST analyses delivers far too little cooling, as at latitudes higher than about 20°N and 20°S the zonally averaged SST's are very close to modern. The full coupled CSM integration does not share this property as it delivers a cooling of approximately 2° that is only weakly dependent on latitude over this range reaching a maximum level within this range of latitude of approximately 3°C. Curve 2 shows the equivalent result which has been extracted

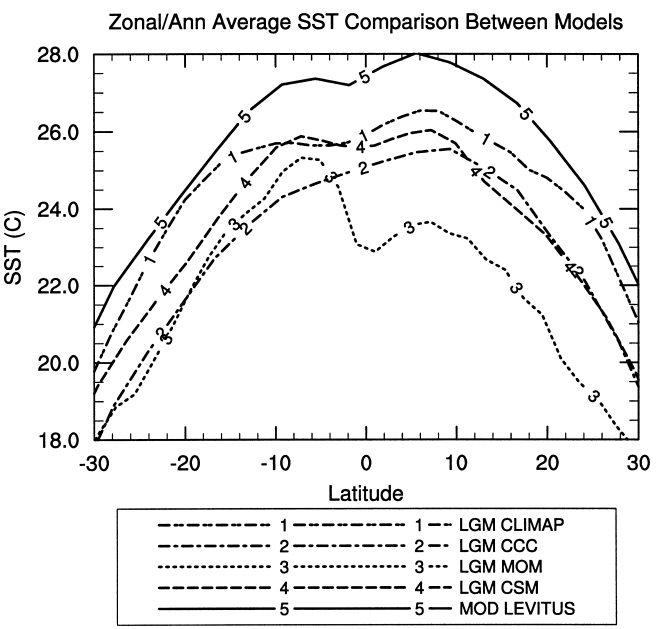

Fig. 7. Zonally averaged SST's in the tropics for the sequence of LGM simulations discussed in the text. Also shown are the modern zonally averaged observed SST's based upon Levitus data.

from the recent LGM integration described by Vettoretti *et al*. (2000) that was based upon the use of the mixed layer ocean coupled AGCM of the Canadian Climate Centre for Modelling and Analysis (CCC2) model. It delivers tropical SST's that are somewhat lower than predicted by the full coupled version of the CSM in the southern hemisphere but essentially identical results in the northern hemisphere. The final result shown on Fig. 7 is that based upon analyses by Bush and Philander (1998) who employed the Princeton coupled atmosphere-ocean model to perform a single decade of integration from initial conditions for which the oceans were assumed to be at rest and therefore for which only the wind driven circulation of the oceans could have come close to equilibrating. Otherwise this model was also run using the Peltier (1994, 1996) surface boundary conditions. The simulations labelled 2 and 4 should therefore be the most accurate and of these two that numbered 4, based upon the full coupled CSM, would have to be preferred since ocean heat fluxes are computed self-consistently as opposed to remaining specified as they are in the CCC2 mixed layer ocean model. However, it will be noted by inspection of the spin-up of this model shown on Fig. 5, that the model was continuing to cool after the 80 year spin-up had been completed. Furthermore, the deep circulation could not have equilibrated by this time, a fact that may be connected to the continued cooling displayed in curve 4. Since the attempt to reach equilibrium using the method for accelerated convergence that the model allows resulted in a marked warming of the planet that may have been due to the violation of energy conservation by the acceleration procedure, we cannot expect the accelerated run to be providing useful information. Our best estimate of the degree of LGM tropical cooing based upon these analyses is approximately 2°C. This most probably represents a lower bound on the degree of tropical cooling that would be characteristic of the fully equilibrated state.

Referring to the review of the proxy data based reconstructions of tropical SST's discussed at the end of Section 2, the 2°C cooling of tropical SST's predicted as a lower bound on cooling using the synchronously coupled version of the NCAR CSM agrees very well with the degree of cooling that has been inferred on the basis of the alkenone "thermometer" (Bard *et al*., 1997). However, it remains an unresolved question as to whether, and if so by how much, the synchronously coupled simulation performed with the NCAR CSM would continue to cool if it were to be integrated into a true statistical equilibrium state. Longer runs of the full coupled model will be described elsewhere.

One final item that warrants discussion by way of conclusion in this paper concerns the modification of the global thermohaline circulation that is predicted by the two fully coupled runs of the NCAR CSM that have been performed to simulate LGM conditions. To this end Fig. 8 shows the zonally averaged overturning streamfunction over all ocean basins for the modern circulation, for the LGM circulation from the 80 year spin-up of the CSM and from the simulation which employed the end condition of the 80 year spin-up to initiate a 50 year period of integration of accelerated integration in which the abyssal ocean was evolved over a period of 2500 years, followed by a further 50 years of synchronously coupled integration. These results for the overturning streamfunction are shown

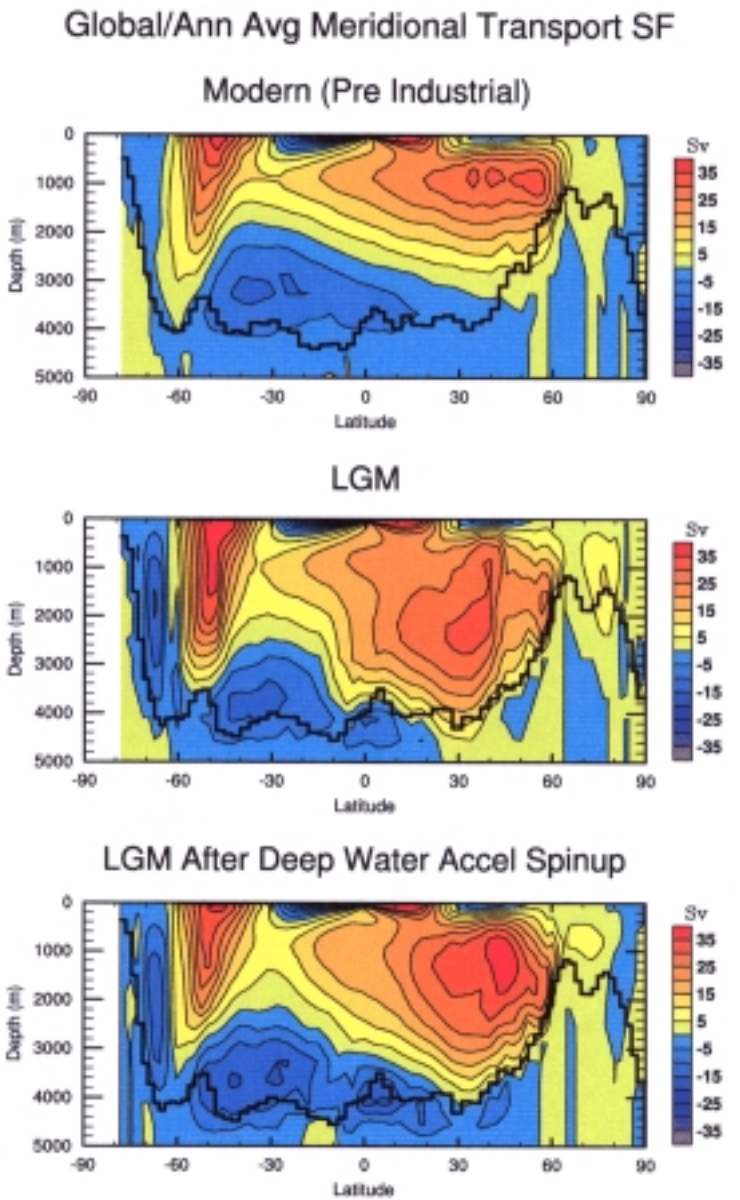

Fig. 8. Zonally averaged overturning streamfunction for the modern, LGM and LGM accelerated versions of the CSM integrations discussed in the text.

respectively in plates (a), (b) and (c) of Fig. 8, the former displaying the result for the modern circulation, (b) showing the result obtained at the end of the 80 year synchronous integration and (c) showing the further modification delivered following the period of accelerated spin-up of the deep circulation.

The results displayed in this figure are the most important contained in the present paper. Inspection of part (a) of the figure demonstrates that the strength and form of the overturning circulation in the Atlantic basin is reasonably well captured by the model although the intensity, measured in Sv on the figure ($1\ Sv = 10^6\ m^3/s$), is somewhat excessive. The overturning circulation is strongly dominated by the process of North Atlantic Deep Water (NADW) formation. However, the NADW formation process does not lead to the penetration of cold, saline NADW to the floor of the basin. Rather, because of the loss of negative buoyancy caused by the manner in which the bottom boundary condition in the vicinity of the sill is handled, as is well known, the overturning circulation does not fully penetrate into the abyss. Part (b) of this figure shows the overturning streamfunction zonally averaged over all basins that obtains at the end of the 80 year synchronous spin-up of the fully coupled model under LGM conditions. Most evident in this result is that the overturning circulation in the northern hemisphere, again dominated by the Atlantic basin, extends to much greater depth than does that in the modern climate system. This is an entirely expected consequence of the fact that the region of deep water formation in the Atlantic is significantly shifted to lower latitudes, and that at these lower latitudes there is no topographic inhibition of the negatively buoyant cold and salty water whose convective downwelling is responsible for NADW formation. This southern shift of the region of deep water formation under LGM conditions takes place in concert with a southern shift in the trajectory of the Gulf Stream. That the trajectory of the Gulf Stream is known to have shifted southwards under LGM conditions is in close accord with paleoceanographic reconstructions of the LGM state of the Atlantic Ocean (e.g. Ruddiman and McIntyre, 1984). It is equally interesting to note, however, that the strength of the overturning cell that is driven by NADW formation is not weaker than that characteristic of the modern circulation. This result is in extreme disagreement with inferences based upon the Ca/Cd proxy for the strength of the overturning circulation that was actually characteristic of the LGM Atlantic Ocean (Boyle and Keigwin, 1987). Plate (c) of this figure shows that this result is not significantly altered when the solution shown in Part (b) is subjected to a prolonged period of accelerated spin-up of the abyssal ocean. A further point of interest, however, concerns the significant intensification of the process of Antarctic Bottom Water (AABW) formation. The strength of this process appears to be quadrupled in the LGM climate simulations that we have performed over that which is characteristic of modern climate conditions.

Although much more detailed diagnostic analyses of these LGM simulations will be required to more fully understand their implications, it is perhaps useful to comment on the possible explanation as to why the NADW formation process is not significantly reduced under LGM climate conditions. It may well be that the

fresh water flux that is being delivered to the surface of the North Atlantic Ocean in these experiments is simply not representative of that which actually occurred at that time. This would be an expected consequence of the fact that the flux due to melting icebergs has not been represented in the sequence of integrations we have performed. That this contribution to "effective " Precipitation-Evaporation (P-E) is liable to play an important role in controlling the strength as well as the time dependence of the overturning circulation will be clear on the basis of evidence of intense iceberg melting events (Heinrich, 1988) that is present throughout the North Atlantic basin on the basis of evidence from deep sea sedimentary cores. Recent detailed theoretical analyses have suggested that this additional contribution to the freshwater flux may play a fundamental role in large scale ocean dynamics (e.g. Sakai and Peltier, 1995, 1996, 1997, 1999). Based upon an accurate reconstruction of LGM sea surface salinity such as that recently provided on the basis of transfer function analyses of isotopic measurements on dinoflagellate cysts (de Vernal *et al*., 2000), it should be possible to employ these observations to infer the strength of the additional freshwater forcing that must have been derivative of the melting of icebergs. Analyses of this kind will be described in detail elsewhere.

CONCLUSIONS

The discussion of recent simulations of LGM climate provided in the preceding section of this paper has illustrated the level of disagreement which continues to exist between the many different models that have been employed to reconstruct the climate that existed during this interesting epoch of Earth history. In the context of the PMIP set of model-model intercomparisons based upon the use of mixed layer ocean coupled AGCM's, for example, tropical SST anomalies are found to vary from a low of –.75°C for the UGAMP model to a high of –3.4°C for the CCC2 model (see Fig. 2). Similarly, tropical land surface temperature anomalies were found to vary from a low of –1.2°C (UGAMP) to a high of –5.3°C (CLIMBER2). In order to begin to reduce the uncertainty connected to model predictions of the state of LGM climate it seems clear that we must begin to work with models in which the dynamics of the oceans are fully taken into account. To this end we have described an initial set of LGM climate reconstructions performed using the recently constructed NCAR Climate System Model (CSM). Although we have yet to obtain a fully equilibrated solution for LGM climate based upon this model, the solutions presented herein have a number of characteristics that appear to be in rather close accord with paleoceanographic inferences, including a significant southward drift of the region of deep water formation in the northern part of the Atlantic Basin and significant increase in the strength of AABW formation. There are also properties of this LGM climate simulation that are discordant with paleoceanographic inferences, however, perhaps foremost among which is the apparently excessive strength of the NADW formation process. We have suggested that this may be due to an underestimate by the model of the freshwater flux acting upon the high latitude North Atlantic

due to the fact that the addition to the buoyancy flux related to the melting of icebergs has yet to be taken into account. It is expected that recent inferences of the sea surface salinity of the high latitude LGM Atlantic by de Vernal *et al*. (2000) might be employed to infer the magnitude of this additional contribution to the buoyancy flux and thereby enable the model to make a definitive prediction of the strength of the NADW formation process that may be compared to existing paleoceanographic inferences. Analyses of this kind are underway and will be described elsewhere.

REFERENCES

Bard, E., F. Rostek and C. Sonzongni, 1997: Interhemispheric synchrony of the last deglaciation inferred from alkenone paleothermometry. *Nature*, **385**, 707–710.

Barnola, J. M., D. Raynaud, Y. S. Korotkevich and C. Lorius, 1987: Vostock ice core provides 160,000-year record of atmospheric CO_2. *Nature*, **329**, 408–418.

Boyle, E. A. and L. Keigwin, 1987: North Atlantic thermohaline circulation during the past 20,000 years linked to high-latitude surface temperature. *Nature*, **330**, 35–40.

Broecker, W., 1997: Mountain glaciers: Recorders of atmospheric water vapour content? *Global Biogeochem. Cycles*, **11**, 589–597.

Bush, A. B. G. and S. G. H. Philander, 1998: The role of ocean-atmosphere interactions in tropical cooling during the last glacial maximum. *Science*, **279**, 1341–1344.

Clark, J. A., W. E. Farrell and W. R. Peltier, 1978: Global changes in postglacial sea level: A numerical calculation. *Quat. Res*., **9**, 265–287.

CLIMAP Project Members, 1976: The surface of the ice-age Earth. *Science*, **191**, 1131–1137.

de Vernal, A., C. Hillaire-Marcel, J.-L. Tureon and J. Matthiessen, 2000: Reconstruction of sea-surface temperature, salinity, and sea ice cover in the northern North Atlantic during the last glacial maximum based on dynocyst assemblages. *Can. J. Earth Sci*., **37**, 725–750.

Farrell, W. E. and J. A. Clark, 1976: On postglacial sea level. *Geophys. J. Roy. astr. Soc*., **46**, 647–667.

Guilderson, T. P., R. G. Fairbanks and J. L. Rubenstone, 1994: Tropical temperature variations since 20,000 years ago: Modulating interhemispheric climate change. *Science*, **263**, 663–665.

Hays, J. D., J. Imbrie and N. J. Shackleton, 1976: Variations in the earth's orbit: Pacemaker of the ice-ages. *Science*, **194**, 1121–1132.

Heinrich, H., 1988: Origin and consequences of cyclic ice rafting in the Northeast North Atlantic Ocean during the past 130,000 years. *Quat. Res*., **29**, 142–152.

Hostetler, S. W. and A. C. Mix, 1999: Reassessment of ice-age cooling of the tropical ocean and atmosphere. *Nature*, **399**, 673–676.

Joussaume, S. and K. E. Taylor, 1995: Status of the Paleoclimate Modelling Intercomparison Project (PMIP). *Proceedings of the First International AMIP Scientific Conference*, WCRP Report 92, WMO Press, Geneva, pp. 425–430.

Marshall, S. J., L. Tarasov, G. K. C. Clarke and W. R. Peltier, 2000: Glaciological reconstruction of the Laurentide ice sheet: physical processes and modelling challenges. *Can. J. Earth Sci*., **37**, 769–793.

Milankovitch, M., 1941: *Canon of Insolation and the Ice Age Problem* (translated from German). U.S. Department of Commerce, Israel Program for Scientific Translations (distr. by Davey, Hartford, Connecticut, 1969).

Mitrovica, J. X. and W. R. Peltier, 1991: On postglacial subsidence over the equatorial oceans. *J. Geophys. Res*., **96**, 20053–20071.

Peltier, W. R., 1974: The impulse response of a Maxwell Earth. *Rev. Geophys. Space Phys*., **12**, 649–669.

Peltier, W. R., 1976: Glacial isostatic adjustment II: The inverse problem. *Geophys. J. Roy. astr. Soc*., **46**, 669–706.

Peltier, W. R., 1994: Ice-age paleotopography. *Science*, **265**, 195–201.
Peltier, W. R., 1996: Mantle viscosity and ice-age ice-sheet topography. *Science*, **273**, 1359–1364.
Peltier, W. R., 1998a: Postglacial variations in the level of the sea: Implications for climate dynamics and solid Earth geophysics. *Rev. Geophys.*, **36**, 603–689.
Peltier, W. R., 1998b: "Implicit ice" in the global theory of glacial isostatic adjustment. *Geophys. Res. Lett.*, **25**, 3957–3960.
Peltier, W. R. and J. T. Andrews, 1976: Glacial isostatic adjustment I: the forward problem. *Geophys. J. Roy. astr. Soc.*, **46**, 605–646.
Peltier, W. R., W. E. Farrell and J. A. Clark, 1978: Glacial isostasy and relative sea level: a global finite element model. *Tectonophysics*, **50**, 81–110.
Pinot, S., G. Ramstein, S. P. Harrison, I. C. Prentice, J. Guiot, M. Stute and S. Joussaume, 1999: Tropical paleoclimates at the Last Glacial Maximum: comparison of Paleoclimate Modeling Intercomparison (PMIP) simulations and paleodata. *Clim. Dyn.*, **15**, 857–874.
Rind, D. and D. Peteet, 1995: Terrestrial conditions at the last glacial maximum and CLIMAP sea-surface temperature estimates: Are they connected? *Quat. Res.*, **24**, 1–22.
Rostami, K., W. R. Peltier and A. Mangini, 2000: Radiometric dating of Quaternary marine terraces, sea level changes and uplift history of Eastern Patagonia, Argentina: Comparisons with predictions of the ICE-4G (VM2) model of the global process of glacial isostatic adjustment. *Quat. Sci. Rev.*, **19**, 1495–1525.
Ruddiman, W. F. and A. McIntyre, 1984: Ice-age thermal response and climatic role of the surface North Atlantic Ocean, 43°–63°N. *Geological Society of America Bulletin*, **95**, 381–396.
Sakai, K. and W. R. Peltier, 1995: A simple model of the Atlantic thermohaline circulation: internal and forced variability with paleoclimatological implications. *J. Geophys. Res.*, **100**, 13455–13479.
Sakai, K. and W. R. Peltier, 1996: A multi-basin reduced model of the global thermohaline circulation: paleoceanographic analyses of the origins of ice-age climate variability. *J. Geophys. Res.*, **101**, 22535–22562.
Sakai, K. and W. R. Peltier, 1997: Dansgaard-Oeschger oscillatons in a coupled atmosphere-ocean climate model. *J. Climate*, **10**, 949–970.
Sakai, K. and W. R. Peltier, 1999: A dynamical systems model of the Dansgaard-Oeschger oscillation and the origin of the Bond cycle. *J. Climate*, **12**, 2238–2255.
Schrag, D., G. Hampt and D. Murray, 1996: Pore fluid constraints on the temperature and oxygen isotopic composition of the glacial ocean. *Science*, **272**, 1930–1931.
Shackleton, N. J., 1967: Oxygen isotope analyses and Pleistocene temperatures re-addressed. *Nature*, **215**, 15–17.
Spero, H., D. L.Bijma and B. Bemis, 1997: Effect of seawater carbonate concentration on foraminiferal carbon and oxygen isotopes. *Nature*, **390**, 497–500.
Stute, M., M. Forster, H. Frischkorn, A. Serejo, J. F. Clark, P. Schlosser, W. S. Broecker and G. Bonani, 1995: Cooling of tropical Brazil during the last glacial maximum. *Science*, **269**, 379–383.
Tarasov, L. and W. R. Peltier, 1999: The impact of thermomechanical ice-sheet coupling on a model of the 100 kyr ice-age cycle. *J. Geophys. Res.*, **104**, 9517–9545.
Thompson, L. E., E. Mosley-Thompson, M. E. Davis, P. N. Lik, K. A. Henderson, J. Cole-Dai, J. F. Bolzen and K. B. Liu, 1995: Late glacial stage and Holocene tropical ice ocre records from Huascaran, Peru. *Science*, **269**, 46–50.
Tushingham, A. M. and W. R. Peltier, 1991: ICE-3G: A new global model of late Pleistocene deglaciation based upon geophysical predictions of post-glacial relative sea level change. *J. Geophys. Res.*, **96**, 4497–4523.
Tushingham, A. M. and W. R. Peltier, 1992: Validation of the ICE-3G model of Wurm-Wisconsin deglaciation using a global data base of relative sea level histories. *J. Geophys. Res.*, **97**, 3285–3304.
Vettoretti, G., W. R. Peltier and N. A. McFarlane, 2000: Global water balance and atmospheric water vapour transport at Last Glacial Maximum: Climate simulations with the CCCma atmospheric

general circulation model. *Can. J. Earth Sci*., **37**, 695–723.
Wu, P. and W. R. Peltier, 1982: Viscous gravitational relaxation. *Geophys. J. Roy. astr. Soc*., **70**, 435–485.
Wu, P. and W. R. Peltier, 1984: Pleistocene deglaciation and the Earth's rotation: a new analysis. *Geophys. J. Roy. astr. Soc*., **76**, 202–242.

W. R. Peltier (e-mail: peltier@atomosp.physics.utoronto.ca) and L. P. Solheim